Ⅲ-3

Chemistry

Highlight

BL3U

Microfluidics of Liquid Mixtures for Soft X-ray Absorption Spectroscopy

M. Nagasaka[1, 2], A. A. Vu[1, 3], H. Yuzawa[1], N. Takada[1], M. Aoyama[1], E. Rühl[3] and N. Kosugi[1, 2]

[1]*Institute for Molecular Science, Okazaki 444-8585, Japan*

[2]*SOKENDAI (The Graduate University for Advanced Studies), Okazaki 444-8585, Japan*

[3]*Physikalische Chemie, Freie Universität Berlin, Takustr. 3, D-14195 Berlin, Germany*

Microfluidics is a chemical technique to realize highly efficient chemical reactions in liquid phase [1]. Recently, X-ray diffraction in the hard X-ray region has been used for a variety of systems by using microfluidics [2]. However, it is difficult to apply spectroscopic techniques in the soft X-ray region since soft X-rays cannot penetrate a microfluidic cell. Previously, we developed a microfluidic cell for soft X-ray absorption spectroscopy (XAS) of structured liquids [3]. In this study, we have successfully observed a laminar flow between pyridine and water in soft X-ray fluorescence image by improving a microfluidic cell and measured N K-edge XAS in the mixed part of microfluidics to reveal the interaction between water and pyridine in a laminar flow.

The experiments were performed at the BL3U connected to a custom-made microfluidic cell. A T-shape microfluidics setup with the width of 50 μm is made from PDMS resin which is covered by a 100 nm Si_3N_4 membrane. Pyridine and water are mixed in the microfluidics with flow rates of 4 μl/min by using syringe pumps. The ultrahigh vacuum of the soft X-ray beamline is separated from the microfluidic cell that is kept at atmospheric helium pressure by a 100 nm thick SiC membrane with a window size of 30 × 30 μm^2. This window determines the photon beam size [4]. Spatially resolved XAS spectra of the microfluidic cell are measured in the fluorescence yield mode at around 320 eV to 430 eV in N K-edge and at 460 eV to 580 eV in O K-edge, respectively, by using a silicon drift detector.

Figure 1 shows a soft X-ray fluorescence image of the T-shape microfluidic cell excited by soft X-rays at 550 eV. Pyridine (*P*) flows from the upper side, and water (*W*) from the lower side. The water-pyridine mixture (*M*) flows to the right-hand part after the junction of the liquids. Since 550 eV is above the O K-edge, the fluorescence shows high intensity due to water and low intensity at pyridine, respectively. The laminar flow of water and pyridine is observed in the mixed part of the microfluidics.

Figure 2 shows N K-edge XAS spectra at different positions in the mixed part shown in Fig. 1, where the horizontal position is fixed to X = 600 μm and the vertical positions are scanned. From the intensity of the N 1s → π* transition, the center position of the mixed part is at Y = 504 μm. By changing the position from pyridine (Y = 540 μm) to the water part (Y = 460 μm), the π* peak shows a spectral shift to the higher photon energy due to the formation of the pyridine-water mixtures [5]. This shift abruptly occurs at Y = 500 μm, indicating clearly the phase separation in the laminar flow.

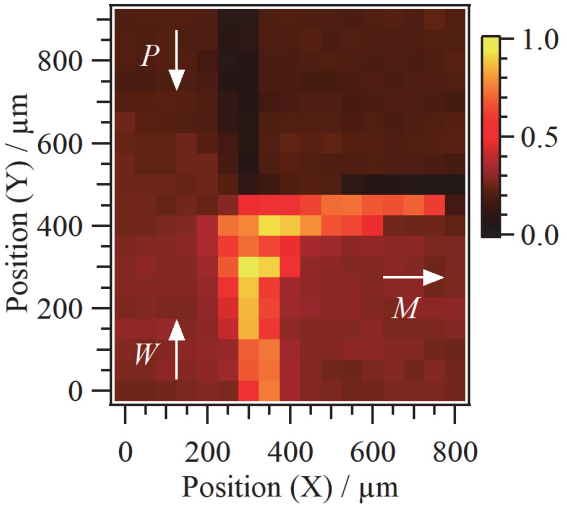

Fig. 1. Soft X-ray fluorescence image of a T-shaped microfluidic cell excited by soft X-rays at 550 eV. A laminar flow is observed in the mixed part.

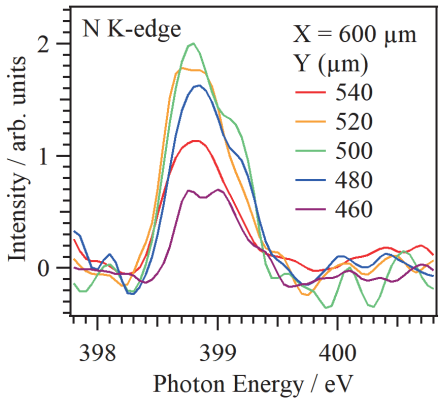

Fig. 2. N K-edge XAS spectra at different positions in the mixed part of the microfluidic flow shown in Fig. 1. The horizontal position is fixed to X = 600 μm, and the vertical position is scanned in the mixed part.

[1] T. Kitamori *et al.*, Anal. Chem. **76** (2004) 53.
[2] B. Weinhausen and S. Köster, Lab Chip **13** (2013) 212.
[3] M. Nagasaka *et al.*, UVSOR Activity Report **2016** (2017) 106.
[4] M. Nagasaka *et al.*, J. Electron Spectrosc. Relat. Phenom. **224** (2018) 93.
[5] M. Nagasaka *et al.*, Z. Phys. Chem. *in press*.

BL1U

Molecular Orientation Induced by Irradiation UV to Achiral Dinuclear Schiff Base Metal Complexes-PVA Hybrid Materials

T. Akitsu[1], H. Nakatori [1], S. Yagi[1], H. Sato[1], T. Soejima[1], S. Yamazaki[1], D. Tadokoro[2], M. Fujiki[3], M. Fujimoto[4] and M. Katoh[4]

[1]*Faculty of Sciences, Tokyo University of Science, Tokyo 162-8601, Japan*
[2]*Graduate School of Human and Environmental Studies, Kyoto University, Kyoto 606-8501, Japan*
[3]*Graduate School of Materials Sciences, NAIST, Nara 630-0192, Japan*
[4]*UVSOR Synchrotron Facility, Institute for Molecular Science, Okazaki 444-8585, Japan*

In recent years, studies on optical vortex light have attracted attention. A light vortex having a spiral wavefront and carrying an orbital angular momentum gives a torque when irradiated on an object. As a result, a phenomenon which cannot be observed with ordinary light is expected. In fact, applied research on azo polymers has been reported.

We have attempted molecular orientation control by irradiating linearly and circularly polarized ultraviolet light to a polymer film in which an azo-dye that undergoes a photoisomerization reaction with a Schiff base metal complex is dispersed [1]. Previous research has revealed that it aligns in one direction by irradiation with linearly polarized ultraviolet light and spirally aligns by irradiation with circularly polarized ultraviolet light. Herein, the purpose of this research is to investigate what will happen if light vortex is irradiated on the complex we have studied so far.

We measured UV-vis spectra of **MO** (methyl orange, azo-dye), **ZnL** (Fig. 1), **ZnL+MO** in PVA (polyvinyl alcohol) aqueous solution. An absorption peak was observed in the vicinity of 280 nm in all the samples. Therefore, the irradiation wavelength of the optical vortex was set to 280 nm. Photo-illumination (both circularly polarized light and optical vortex) of UV light was carried out using UVSOR BL1U.

Prior to actual experiments, we have investigated only PVA films to remove effects of artifact CD peaks due to LD of oriented samples. Difference CD spectra PVA films before and after optical vortex (270 nm, l=-1, 1) irradiation corresponding to the π-π* band of acetate groups were carefully confirmed to disappear artifact CD peaks just like Fig. 2.

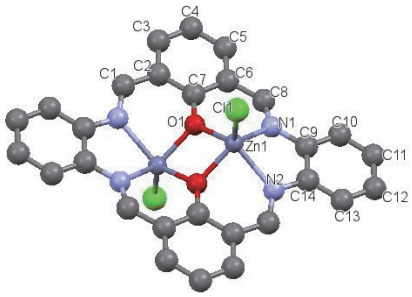

Fig. 1. Crystal structure of **ZnL** from PXRD data.

As shown in Figs. 3 and 4, not only **ZnL+MO** (due to Weigert effect) but also only **ZnL** (due to orbital angular momentum) could be successfully observed to appear CD peaks after optical vortex irradiation.

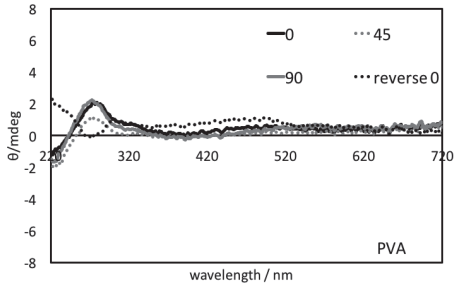

Fig. 2. CD spectra 0°, 45°, 90° reverse side of PVA cast film after optical vortex (280 nm, l=-1) irradiation.

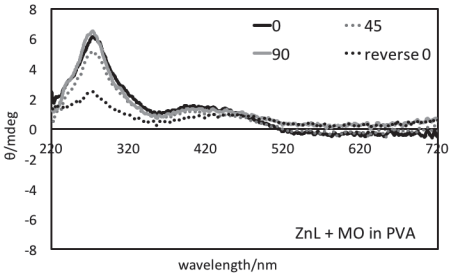

Fig. 3. CD spectra 0°, 45°, 90° reverse side of PVA cast film containing **ZnL+MO** after optical vortex (280 nm, l=-1) irradiation.

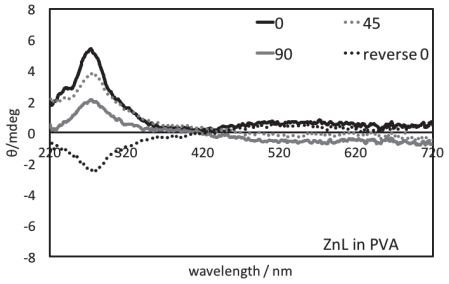

Fig. 4. CD spectra 0°, 45°, 90° reverse side of PVA cast film containing **ZnL** after optical vortex (280 nm, l=-1) irradiation.

[1] N. Sunaga, T. Akitsu, T. Konomi and M. Katoh, MATEC Web of Conferences **130** (2017) 07004.

BL3U, BL4U

XAS Characterizations on NaOH Solutions and Calcium Chlorides in Transmission Mode

Y.-S. Liu[1], P.-A. Glans[1], J. Guo[1], M. Nagasaka[2], T. Ohigashi[2] and N. Kosugi[2]
[1]*Lawrence Berkeley National Laboratory, 1 Cyclotron Road, Berkeley, CA 94720, USA*
[2]*Institute for Molecular Science, Okazaki 444-8585, Japan*

The electronic structure of ion solvated in liquids has long been studied owing to its importance in many applications. The related ionic and electronic transportation mechanisms are still far from understood in the microscopic scales, which are crucial for the broad applications ranging from bioscience, pharmacology and energy science such as metal ion batteries.

Here, we are reporting our preliminary results taken at UVSOR in 2016 and 2017 on O K-edge XAS in NaOH solutions and Ca L-edge in $CaCl_2$ solutions in different solvents (water, methanol and ethanol). The results show that the in-situ capabilities are promising at UVSOR beamlines, especially in transmission mode really provide high quality XAS spectra and stability.

Figure 1 left shows the O K-edge XAS that are taken at UVSOR from the concentrated NaOH solutions. The results are showing that the solvated OH- anion group gives a spectroscopic signature feature at around 532 ~ 533 eV (see enlarged Fig.1 right). This feature has intensity change depending on the concentration corresponding to the increasing of OH- content in the solutions. Most importantly, these results are consistent with our previous experimental study using fluorescence and electron-yield mode measurements at the other synchrotron facilities. In addition, the theoretical calculated XAS spectra of NaOH solutions are to be completed for understanding the ion solvation shell. The results taken at UVSOR could be extremely helpful as the XAS spectra obtained from the transmission geometry removes the so-called saturation effect, which is often been questioned in fluorescence mode.

Figure 2 shows the Calcium L-edge spectra of 1 Molar $CaCl_2$ in different solvents (water, methanol and ethanol). The experimental Ca L-edges spectra are extremely sensitive to its solvents. However, since Ca^{2+} has a $3d_0$ configuration, the pronounced differences between solvents indicating that the polar solvent, i.e. water vs. methanol, plays an important role to its electronic structure. The main differences can be seen from the variation of pre-peak intensities around 348.4 and 351.4 eV. However, the detail solvation shells need to be confirmed and incorporate with theoretical calculations.

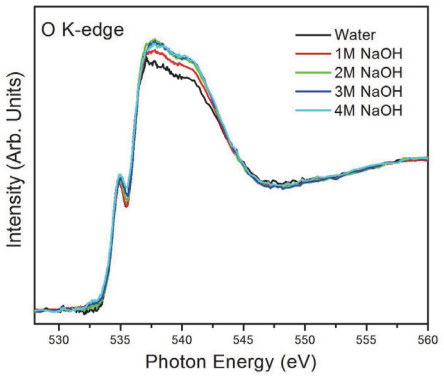

Fig. 1. O K-edge XAS spectra of different concentration NaOH solutions.

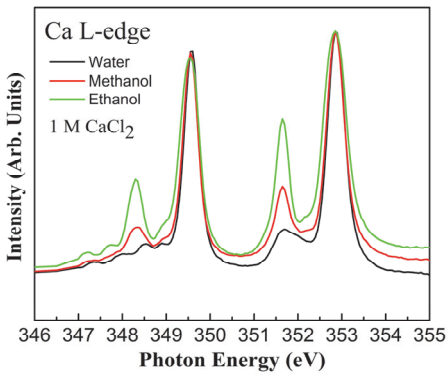

Fig. 2. Ca L-edge XAS spectra in different solvents.

BL3U

Soft X-ray Absorption Spectroscopy of 4-Cyano-4'-pentylbiphenyl Molecules in Liquid, Liquid-crystal and Solid Phases

H. Iwayama[1, 2]

[1]*UVSOR Synchrotron Facility, Institute for Molecular Science, Okazaki 444-8585, Japan*

[2]*School of Physical Sciences, The Graduate University for Advanced Studies (SOKENDAI), Okazaki 444-8585, Japan*

The liquid crystal is one of the most important materials for display devices. In the case of nematic liquid crystals, the rod-shaped organic molecules have no position order, but they self-align to have long-range directional order with their long axes roughly parallel. Since X-ray absorption fine structure (XAFS) spectroscopy is sensitive to a local atomic geometry and the chemical state of the atom of one specific element, XAFS spectroscopy is suitable to investigate structures of liquid crystals materials. However, XAFS measurement of liquid crystal materials is limited to one in a solid phase due to the requirement of high vacuums of a sample chamber. Considering the fact that they work as display device in a liquid-crystal phase, we need to measure XAFS in a liquid-crystal phase. Recently, Nagasaka developed a liquid cell [1], which allows us to measure XAFS spectra of liquid samples. In this work, we measure XAFS of liquid-crystal materials in liquid, liquid-crystal and solid phase with this liquid cell.

Our sample is 4-Cyano-4'-pentylbiphenyl (5cb), which is one of the most popular liquid-crystal materials. A schematic draw of 5cb molecules is shown in Fig. 1. The phase transition temperature of liquid to liquid-crystal and liquid-crystal to solid are 22.5 and 35°C, respectively. The XAFS measurements were carried out at BL3U. After liquid cell which is composed of two Si3N4 membranes was filled with the liquid sample, the thickness of liquid sample was optimized by controlling the He gas pressure around the cell. The photon energy was calibrated by using the C-K edge XAS spectrum of the proline thin layer.

Figure 1 shows C K-edge XANES spectra of 5cb sample at three different temperature, which correspond to liquid, liquid-crystal and solid phases. We observed a strong peak at 285 eV, which correspond to a core excitation of C 1s to π* orbitals of phenyl group. The peak intensities and shapes are different for each phase. Figure 2 shows N K-edge XANES spectra of 5cb molecules. Splitted peaks at 398.7 and 399.5 eV correspond to a core excitation of N 1s to π* orbitals of nitrile group. As well as C K-edge XANES spectra, peak intensities of 1s-to-π* core excitation at N K-edge depend on their phases.

This phase dependence of core excitations reflect the change of molecular alignments between each phases. Our results shows XANES is powerful tool to observe change of a local chemical environment. A more detail analysis is now in progress.

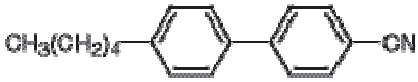

Fig. 1. Schematic draw of 4=Cyano-4'-pentylbiphenl (5cb) molecules.

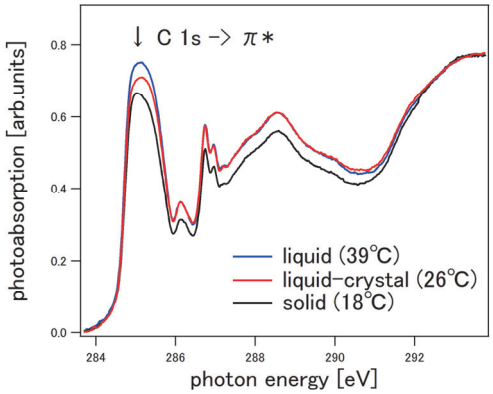

Fig. 2. C K-edge XANES of 5cb molecules at 18 (solid), 26 (liquid-crystal) and 39 °C (liquid).

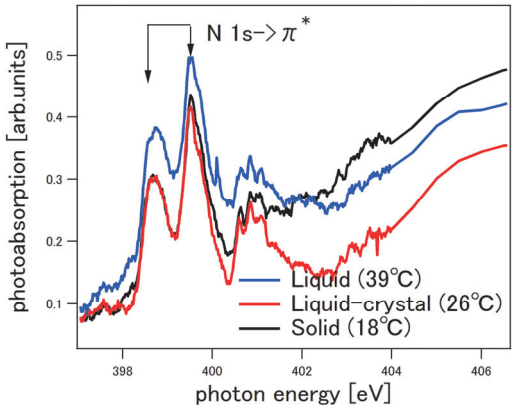

Fig. 3. N K-edge XANES spectra of 5cb samples at 18 (solid), 26 (liquid-crystal) and 39 °C (liquid).

[1] M. Nagasaka, H. Yuzawa and N. Kosugi, J. pectrosc. Relat. Phenom. **200** (2015) 293.

BL3U

Temperature Dependence of Interaction around NO_2^- in Aqueous KNO_2 Solution by Soft X-ray Absorption Spectroscopy

H. Yuzawa[1], M. Nagasaka[1, 2] and N. Kosugi[1, 2]

[1]*Institute for Molecular Science, Okazaki 444-8585, Japan*

[2]*School of Physical Sciences, SOKENDAI (The Graduate University for Advanced Studies), Okazaki 444-8585, Japan*

Understanding of interactions in aqueous electrolyte solutions is one of the highly attractive research subjects [1]. Recently, our research group has studied the interaction between some cations and water by using O K-edge soft X-ray absorption spectroscopy (XAS) of water in the transmission mode [2]. In the present study, we have investigated the temperature dependence of the interaction around the NO_2^- anion by N and O K-edge XAS.

XAS spectra were measured at BL3U equipped with the liquid cell system in the transmission mode [3]. Aqueous KNO_2 solution sample (Molar ratio is KNO_2 : H_2O = 1 : 42.6) was prepared by using the commercial reagent without further purification. After the liquid cell which is composed of two Si_3N_4 membranes and Teflon spacer was filled with the sample, the thickness of the liquid cell was optimized by controlling the He pressure around the cell and N or O K-edge XAS was measured. Temperature in the cell (0 − 70°C) was controlled by the circulation of a liquid heat carrier by using a thermo-chiller, and it is monitored by a thermopile. The photon energy was calibrated by the spectrum of the thin polymer film.

Figure 1 shows N and O 1s → π* peaks of NO_2^- in the aqueous KNO_2 solution at various temperatures. In both the N and O K-edges (Fig.1a, b), the shape of the observed peaks such as half width is not changed by heating from 0 to 70°C. On the other hand, the peak energy shift shows a different behavior to each other. Fig. 2 shows the temperature dependence of the observed peak top energy shift. In the N K-edge XAS, the peak top energy is almost constant, indicating that the interaction around N atoms in NO_2^- is hardly influenced by the investigated temperatures. In the O K-edge XAS, the peak top energy is constant until 40°C, but shows a sudden shift to the lower energy with increasing the temperature from 50 to 70°C.

To investigate this phenomenon in detail, we have also done two types of O K-edge XAS experiments; one is the concentration dependence at 25°C and the other is the temperature dependence by using the concentrated aqueous KNO_2 solution (KNO_2 : H_2O = 1 : 1.7, data not shown). In the former, the peak top energy is also shifted to the lower energy with increasing the concentration to pure solid. Since electrolytes in aqueous solution generally decrease the coordination of H_2O and form aggregated structures with increasing the concentration, the observed lower energy shift in Fig. 2b would correspond to the similar phenomenon, i.e., the decrease of the coordination number of water around NO_2^- in the higher temperature region (50 – 70°C). In the latter, the tendency of the peak energy shift is almost the same as the Fig. 2b. Thus, the observed phenomenon in the temperature dependence of O K-edge XAS, which would arise from the decrease of the H_2O coordination, occur regardless of the formation of KNO_2 aggregate structures.

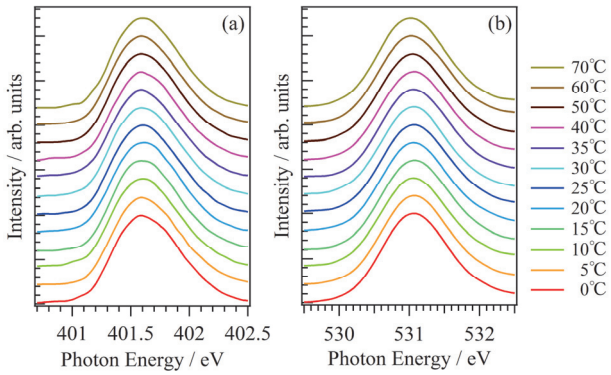

Fig. 1. (a) N K-edge (1s → π*) and (b) O K-edge XAS (1s → π*) peaks of NO_2^- in aqueous KNO_2 solution (KNO_2 : H_2O = 1 : 42.6) at various temperatures (0 – 70°C).

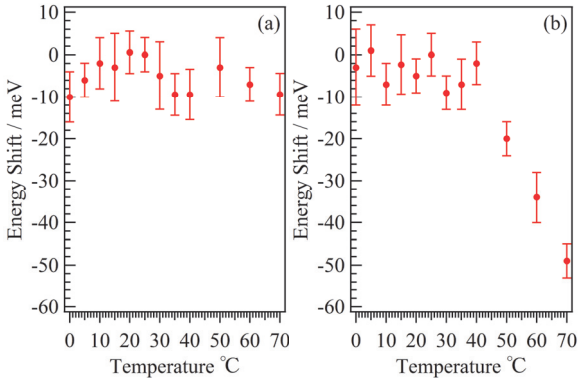

Fig. 2. Temperature dependence of the peak top energy shift in (a) N K-edge and (b) O K-edge XAS from that at 25°C.

[1] Y. Marcus, Chem. Rev. **109** (2009) 1346.
[2] M. Nagasaka *et al*., J. Phys. Chem. B **121** (2017) 10957.
[3] M. Nagasaka *et al*., J. Electron Spectrosc. Relat. Phenom. **224** (2018) 93.

BL4U

Characterization of Meso Porous Monolithic Polymers Containing RAFT Agent by Scanning Transmission X-Ray Microscopy (STXM)

D. Arrua[1], A. Khodabandeh[1], T. Ohigashi[2, 3], N. Kosugi[2, 3] and E. Hilder[1]

[1]*Future Industries Institute, University of South Australia, Building X, Mawson Lakes Campus, GPO Box 2471 Adelaide SA 5001, Australia*

[2]*UVSOR Synchrotron Facility, Institute for Molecular Science, Okazaki 444-8585, Japan*

[3]*School of Physical Sciences, The Graduate University for Advanced Studies (SOKENDAI), Okazaki 444-8585, Japan*

The preparation of hierarchically mesoporous materials exhibiting two or more distinct pore size distributions has found utility in diverse applications, including catalysis and liquid separations [1]. The defining parameters of the 3D network of such system can be adjusted, however this is not a trivial method. Typically, the polymerization is initiated via thermal free radical polymerization which results in the formation of linear polymer chains followed by crosslinking and gelation steps. This mechanism is called polymerization-induced phase separation (PIPS) and the gelation step dictates the resultant morphology and allows for control of the macro- and meso-structure of a continuous piece of porous material known as “monoliths”.

The gelation step can be tuned by using different solvents in the monolith precursor, from well-known organic solvents such as methanol, ethanol and acetone to some less famous large alcohol molecules such as 1-dodecanol. For preparation of percolating macropores, polymeric solvents such as poly(ethylene glycol) with different molecular weights can be used as pore forming materials.

Introducing a RAFT agent (Reversible Addition−Fragmentation chain-Transfer agent) to the above system offered a control over the polymer mechanism as well as on the morphology of the obtained monolithic polymers [2]. Respect to the surface chemistry of the obtained well-defined 3D network, an accurate characterization is required especially when polymeric forming pore agents were utilized [3, 4].

The characterization by STXM of polymeric monolith materials was performed at the BL4U of the UVSOR synchrotron facility. STXM imaging was conducted by focusing on the C 1s core-line signal in NEXAFS. Figure 1 shows the C 1s NEXAFS spectra obtained for three monolithic polymers (A1 with no RAFT agent, A2 and A3 with different amount of RAFT agent). In all these monoliths, polyethylene glycol (PEO *Mw* ~35K) were used as part of pore forming material.

In our first assessment, the components found by STXM were the poly (Sty-co-DVB) monolith domain, and the embedding resin for three different monoliths (A1 to A3, with both 100 nm and 300 nm sections).

The spectrum for the crosslinked styrene-based scaffold has a strong peak at 284.6 eV, which is characteristic of C 1s → π*C=C transition in a phenyl ring. On the other hand, there is no strong peak for residue PEO which is expected to retain in the sample. Considering the size of the polymer globules (~50 nm, estimated by scanning electron microscopy (SEM)) in sample A2 and A3 as well as ~200 nm domain between globules (formed via pore forming agent), the export data via the region method could potentially hide the signal of the PEO residue (pore forming material). This study is now in progress.

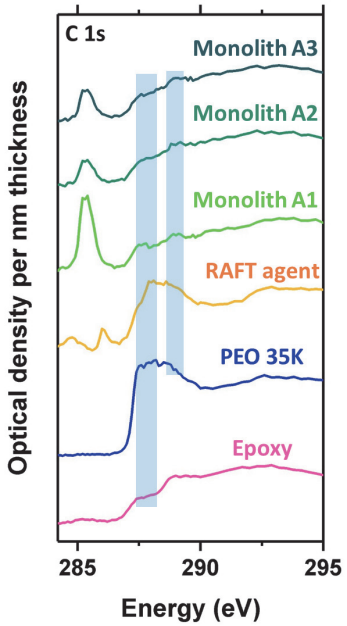

Fig. 1. NEXAFS reference spectra of the epoxy (embedding matrix), PEO Mw ~35K, RAFT agent and polystyrene cross-linked monoliths (A1 with no RAFT agent, A2 with RAFT agent (molar ratio between [Initiator] 1: [RAFT] 1) and A3 with RAFT agent (molar ratio between [Initiator] 1: [RAFT] 2) that correspond to 1 nm thickness of each component.

[1] D. Wu *et al.*, Chem. Rev., **112** (2012) 3959.
[2] K. J. Barlow *et al.*, Poly Chem, **5** (2014) 722.
[3] D. Arrua *et al.*, UVSOR Activity Reports **42** (2014) 76.
[4] A. Khodabandeh *et al.*, Poly Chem, **9** (2018) 213.

BL4B

Metastable CS_2^{2+} States Studied by an Electron-Electron-Ion Coincidence Method

Y. Hikosaka[1] and E. Shigemasa[2]

[1]*Institue of Liberal Arts and Sciences, University of Toyama, Toyama 939-0364 Japan*
[2]*UVSOR Synchrotron Facility, Institute for Molecular Science, Okazaki 444-8585 Japan*

Doubly-charged positive-ions of molecules are energetically unstable due to the Coulomb repulsion between the two positive charges, and they usually undergo rapid dissociations into fragments. Mass spectroscopy has however identified since long ago the existence of metastable molecular dications having lifetimes of the order of at least microseconds. In this work, we have employed a magnetic-bottle electron spectrometer adapted to ion detection, whose description is elsewhere [1], and have performed an electron-electron-ion coincidence study for the S2p Auger decay of CS_2, in order to identify the electronic states of the metastable diaction.

The magnetic-bottle electron spectrometer is equipped with a strong permanent magnet and a long solenoid coil, and an inhomogeneous magnetic field created in the ionization region forms a magnetic mirror to collect the electrons from almost the whole 4π solid angle. An electrostatic retarder, which consists of a 1.3-m long tube and three Mo meshes (94% transmission each), is installed inside the solenoid tube [2]. For coincidence detection of the counterpart ions, a pulsed high voltage was applied to the ionization region, according to an electron-detection, and the formed ions were introduced into the same microchannel plate detector for electron detection.

A multi-electron ion coincidence measurement was made for CS_2 at a photon energy of 321.4 eV (bandwidth of ~150 meV), by applying a retardation of 120 V for electron observations. The top panel of Fig. 1 shows a spectrum of dication states populated after the Auger decay from the S2p core-hole states, which is derived from the energy correlations between photoelectrons and Auger electrons observed in coincidence. The energy resolution allows us to locate different electronic states of CS_2^{2+}, though the vibrational structures known for some specific CS_2^{2+} states are hardly identified. We can examine the ion species produced from these dication states, by inspecting the coincidences among the two electrons and ion(s). The two-dimensional map in Fig. 1 shows the derived correlations, and ion spices formed from the individual dication states are presented. Dominant coincidence with CS_2^{2+} is observed for the low-lying diction states around 26-29 eV, and these states are metastable having lifetimes longer than microsecond order. In contrast, dication states lying above 30 eV dissociate, before arriving the detector, mainly into the fragments of S^+ and CS^+.

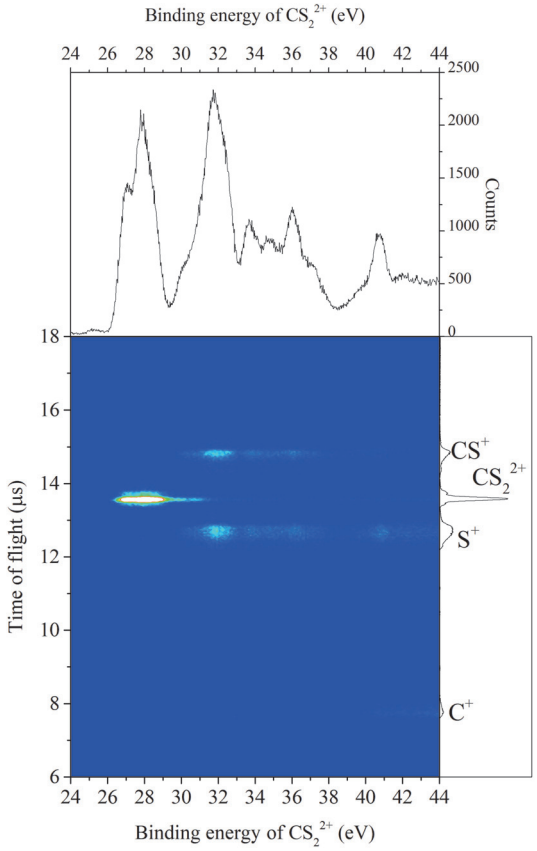

Fig. 1. Two-dimensional map showing the correlations between the CS_2 dication states and time-of-flights of ions, derived from the coincidences among two electrons and ion(s). Top panel shows a spectrum of dication states populated after the Auger decay from the S2p core-hole states. The time-of-flight spectrum of ions is displayed in the right panel.

[1] A. Matsuda *et al.*, Rev. Sci. Instrum. **82** (2011) 103105.
[2] Y. Hikosaka *et al.*, J. El. Spectrosc. Rel. Phemon. **192** (2014) 69.

BL4B

Multi-Electron-Ion Coincidence Spectroscopy: Auger Decay from Xe 4s Core-Hole State

Y. Hikosaka[1] and E. Shigemasa[2]

[1]*Institue of Liberal Arts and Sciences, University of Toyama, Toyama 939-0364 Japan*
[2]*UVSOR Synchrotron Facility, Institute for Molecular Science, Okazaki 444-8585 Japan*

Auger decay from core-hole states in atoms often produces a variety of multiply-charged ions. Multi-electron coincidence spectroscopy, which is effectively achieved by using a magnetic bottle electron spectrometer, is a useful tool to identify the multiple Auger decay pathways, overcoming the ambiguities resulting from the overlap of Auger lines from different core holes. The benefit of this spectroscopy can be significantly increased when the multi-electrons are observed in further coincidence with ions, because different multi-ionization steps can be isolated by the observed ion charges.

In this work, we have performed multi-electron-ion coincidence spectroscopy to study the Auger decay of Xe 4s core-hole state. The multi-electron-ion coincidence spectrometer utilized in this work is based on a magnetic-bottle time-of-flight electron spectrometer with ion detection capability [1], equipped with an electrostatic retarder to improve the energy resolution in electron observations [2]. A similar multi-electron-ion coincidence setup was developed by Eland et al. [3].

A multi-electron ion coincidence measurement was made for Xe at a photon energy of 350 eV (bandwidth of ~90 meV). The black curve in Fig. 1 shows an total Auger electron spectrum observed in coincidence with 4s photoelectron. The formation of the $4d^{-1}5l^{-1}$ states is due to the Coster-Kronig transitions from $4s^{-1}$, and that of $4d^{-2}$ to the super-Coster-Kronig transitions. Structures below 40 eV arise largely from the overlap of the subsequent decays of these $4d^{-1}5l^{-1}$ and $4d^{-2}$ states.

The Auger electron spectra coincident with individual ions are compared in this figure. Clear differences are observed among the spectral features. This observation demonstrates that different Auger pathways are clearly isolated by the coincidence observation including ions. The spectrum coincident with Xe^{3+} ion (shown in red) displays only the structures assignable to the formation of the $4d^{-1}5l^{-1}$ states and their subsequent decays. Since the $4d^{-2}$ states proceed to sequential decays emitting additional two Auger electrons [4], and corresponding structures are isolated in the spectrum coincident with Xe^{4+} ion (blue). The spectrum coincident with Xe^{5+} ion (green), presenting the triple Auger decay of the 4s core-hole state, shows a distribution increasing gradually as decreasing the kinetic energy, where no remarkable Auger structure is seen.

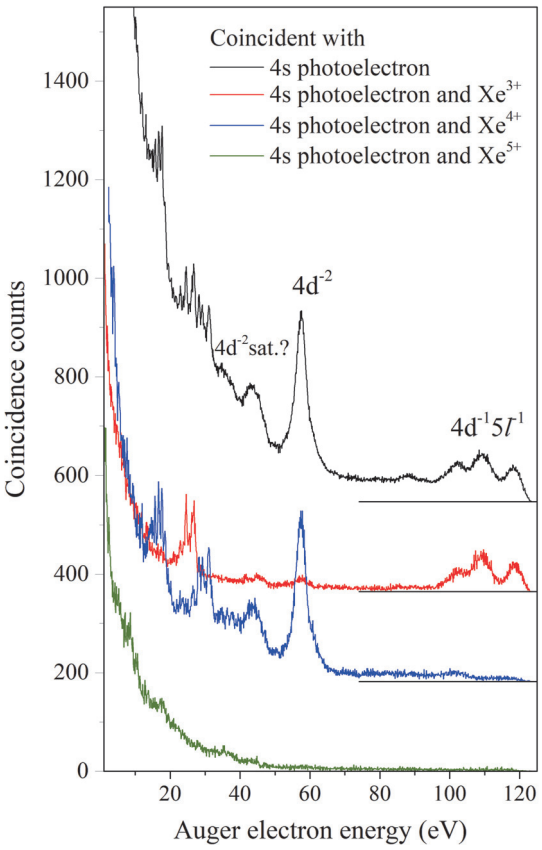

Fig. 1. Auger electron spectrum (balck) observed in coincidence with 4s photoelectron, together with the spectra derived by further coincidence with ions of Xe^{3+} (red), Xe^{4+} (blue) and Xe^{5+} (green).

[1] A. Matsuda *et al.*, Rev. Sci. Instrum. **82** (2011) 103105.
[2] Y. Hikosaka *et al.*, J. El. Spectrosc. Rel. Phemon. **192** (2014) 69.
[3] J.H.D. Eland *et al.*, Chem. Phys. Lett. **548** (2012) 90.
[4] Y. Hikosaka *et al.*, Phys. Rev. Lett. **98** (2007) 183002.

BL5B

Zeeman Quantum Beat in Helium Fluorescence Decay Curve

T. Kaneyasu[1], Y. Hikosaka[2] and H. Iwayama[3, 4]
[1]*SAGA Light Source, Tosu 841-0005, Japan*
[2]*Graduate School of Medicine and Pharmaceutical Sciences, University of Toyama, Toyama 930-0194, Japan*
[3]*UVSOR Synchrotron Facility, Institute for Molecular Science, Okazaki 444-8585, Japan*
[4]*The Graduate University for Advanced Studies (SOKENDAI), Okazaki 444-8585, Japan*

When several quantum paths connect the initial and final states of atomic transition, the quantum interference among these paths may cause quantum beat in the physical observables of the system. The quantum beat has been frequently observed in fluorescence decay following coherent excitation of the atomic and molecular system using lasers [1]. In that case, the laser pulse prepares the atomic system in a coherent superposition of the several states. This method can be applied to the atomic excitation using synchrotron radiation because it may cause coherent excitation of several levels within a bandwidth of the monochromatized light. We planned to use the quantum beat phenomena to study the magnetic sublevel population in the vortex-atom interaction [2]. As a first step of the quantum beat study, we observed the Zeeman quantum beat in helium fluorescence decay curve.

The experimental scheme is shown in Fig. 1. The experiments were performed at BL5B. The fluorescence decay curve was measured using the VUV pulse provided by the single bunch operation of the UVSOR ring. We observed the UV or visible fluorescence following the 1s→*n*p (*n*=4-7) excitation of helium atoms at the VUV wavelength region. A weak magnetic field of several tens of Gauss was applied to the interaction region. The direction of the magnetic field was parallel to the photon propagation axis. This magnetic field induced the Zeeman shift of the magnetic sublevels M_j=±1 which caused the interference in the decay paths. Thus it was expected that the fluorescence decay curves show beat structure which oscillates at frequency 2ω according to the Zeeman shift energy of ħω.

Figure 2 shows the measured decay curves following the 1s→6p excitation. In accordance with the interference model described above, we found that the beat structure was superimposed on the decay curve and its oscillating frequency increased when the solenoid coil current increased. The observed beat frequency agrees well with the Zeeman shift estimated by the magnetic field measurement. Furthermore the beat structure vanished when the magnetic field was parallel to the electric field vector of the VUV pulse (not shown here). This is because the dipole-allowed magnetic sublevel is limited to M_j=0 in this configuration. These results strongly support the reliability of the quantum beat measurement using the synchrotron radiation.

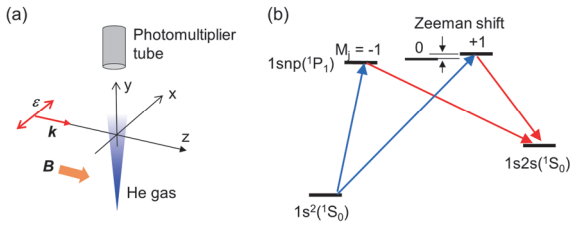

Fig. 1. (a) Experimental setup for observing the helium Zeeman quantum beat. The magnetic field was produced by solenoid coils. Helium atoms were excited by the VUV pulses of 178 ns repetition. The UV or visible fluorescence was detected by a photomultiplier tube. (b) Energy level diagram of the helium atom and excitation/decay pathways in the present study.

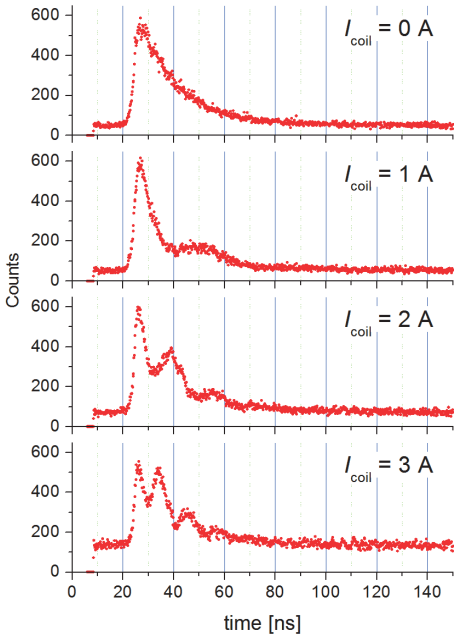

Fig. 2. Fluorescence decay curves of the 1s6p excited state of helium. The wavelength of the excitation pulse was set to 51.2 nm while the wavelength of the fluorescence was 345 nm.

[1] H. Bitto and J.R. Huber, Opt. Comm. **80** (1990) 185.
[2] A. Afanasev *et al.*, Phys. Rev. A **88** (2013) 033841.

BL6U

Mass Spectra of Xenon Difluoride in Coincidence with the F KVV and Xe $M_{45}N_{45}N_{45}$ Auger Electrons

M. Kono[1, 2, 3], F. Yamashita[4], H. Iwayama[5, 6], K. Okada[4] and E. Shigemasa[5, 6]

[1]*School of Science and Technology, Kwansei Gakuin University, Sanda 669-1337, Japan*
[2]*Senri International School of Kwansei Gakuin, Minoh 562-0032, Japan*
[3]*RSPE, Australian National University, Canberra, ACT 2601, Australia*
[4]*Graduate School of Science, Hiroshima University, Higashi-Hiroshima 739-8526, Japan*
[5]*UVSOR Synchrotron Facility, Institute for Molecular Science, Okazaki 444-8585, Japan*
[6]*School of Physical Sciences, The Graduate University for Advanced Studies (SOKENDAI), Okazaki 444-8585, Japan*

Xenon difluoride attracts the attention of X-ray spectroscopists because it has similar binding energies among Xe $3d_{5/2}$, Xe $3d_{3/2}$ and F 1s subshells [1]. Southworth *et al.* [2] have recently measured the partial ion yield curves of XeF_2 and found that the charge state distribution of Xe^{q+} shifts down compared to the Xe atom case. Our previous study [3] has been concerned with the Auger spectra to get an insight into the molecular electronic states leading to the production of Xe^{q+}. The results show that at the σ* resonance the F KV_oV_o peak is most intense, while the Xe $M_5N_{45}N_{45}$ transitions are dominant at the shape resonance. Here the symbol V_o means outer- valence orbitals. By comparison of our results with the study by Southworth *et al.*, there exists a strong correlation between the Auger transitions and fragmentation channels. In order to justify this directly, here we conducted the Auger-electron–photoion coincidence (AEPICO) measurements.

The present experiments were performed on the soft X-ray beamline, BL6U, and its setup has been described elsewhere [4]. In brief, a monochromatized light beam of synchrotron radiation was irradiated at right angles to the effusive beam of the sublimated XeF_2 sample. The pressure of the main chamber was kept at 1.0×10^{-3} Pa during all the measurements. Auger electrons traveling through a double toroidal analyzer tube were detected with a position sensitive detector. Pass energies of the analyzer were set to 400 eV. Each electron detection triggered a pulse of electric field applied across the interaction region, extracting photoions toward a time-of-flight mass spectrometer. The coincidence data were obtained as list-mode files, containing a series of the detected electron positions and the ion-arrival time and positions. The photon energy was set at 707.3 eV in this study.

Mass spectra of the photoions coincident with particular Auger electrons can be obtained by extracting the electron kinetic-energy region of interest from the acquired data. The most abundant photoion is F^+ for both the F KV_oV_o and Xe $M_4N_{45}N_{45}$ regions, while the charge distribution of Xe^{q+} differs from each other. The Xe $M_4N_{45}N_{45}$ AEPICO spectrum is shown in Fig. 1. The maximum yield of Xe^{q+} comes at the trivalent ion, which is in contrast with the atomic Xe case where the exclusive production of Xe^{4+} is observed [5]. Based on the proposed transition channel for the Xe^{4+} production following the $M_{45}N_{45}N_{45}$ Auger process of Xe [5], the lower-charged Xe ions are presumably formed through similar transition channels leading to the electron configurations with the holes in the $5\pi_u$ and $10\sigma_g$ orbitals. Since the latter orbital has an F 2p character, the charge(s) can be put on fluorine as well, accounting for the formation of the F^+ and F^{2+} ions.

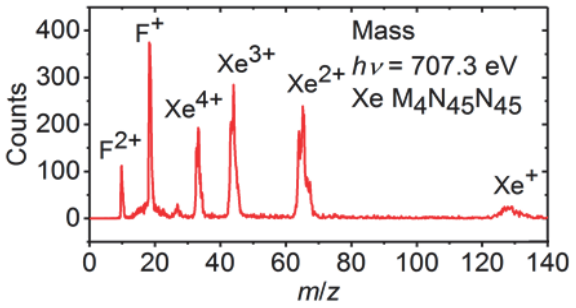

Fig. 1. The photoion mass spectrum of xenon difluoride in coincidence with the Xe $M_4N_{45}N_{45}$ Auger electrons. The spectral data were acquired at the photon energy of 707.3 eV.

[1] T. X. Carroll, R. W. Shaw Jr., T. D. Thomas, C. Kindle and N. Bartlett, J. Am. Chem. Soc. **96** (1974) 1989.
[2] S. H. Southworth, R. Wehlitz, A. Picón, C. S. Lehmann, L. Cheng and J. F. Stanton, J. Chem. Phys. **142** (2015) 224302.
[3] F. Yamashita, M. Kono, H. Iwayama, K. Okada and E. Shigemasa, UVSOR Activity Report **44** (2017) 111.
[4] R. Tateishi, T. Kaneda, H. Iwayama, M. Kono, K. Okada and E. Shigemasa, UVSOR Activity Report **43** (2016) 104.
[5] Y. Tamenori, K. Okada, S. Nagaoka, T. Ibuki, S. Tanimoto, Y. Shimizu, A. Fujii, Y. Haga, H. Yoshida, H. Ohashi and I. H. Suzuki, J. Phys. B: At. Mol. Opt. Phys. **35** (2002) 2799.

BL6U

Site-specific Production of H_3^+ by Core Ionization of CH_3Cl

H. Fujise[1, 2], H. Iwayama[1, 2] and E. Shigemasa[1, 2]

[1]*UVSOR Synchrotron Facility, Institute for Molecular Science, Okazaki 444-8585, Japan*

[2]*School of Physical Sciences, The Graduate University for Advanced Studies (SOKENDAI), Okazaki 444-8585, Japan*

The trihydrogen cation, H_3^+, is an interesting molecule which plays a key role in reactions that lead to complex molecules characterizing interstellar clouds [1]. H_3^+ can be produced from fragmentation reactions of several hydrocarbon molecules using intense laser fields [1], soft X-rays [2], and electron impact [3]. Previous results, irradiating soft X-rays to chloromethane, CH_3Cl, suggested that H_3^+ was preferentially produced and related to the site-specific Auger final states obtained after the core ionization of the Cl 2p electron [4]. However, the detailed production mechanism is still unknown. In this study, we investigate the site-specific production mechanism of H_3^+, and its responsible ionic state of CH_3Cl^{2+}, by core ionization with soft X-rays and Auger-electron-ion coincidence measurements, as well as comparing the results with deuterated chloromethane, CD_3Cl.

Experiments were performed on the soft X-ray BL6U. Radiation from the undulator was monochromatized and focused onto the interaction region of an Auger-electron-ion coincidence spectrometer. The target gas was introduced into the interaction region by effusion from a capillary tube: produced Auger-electrons were energy-analyzed by the double toroidal analyzer (DTA). Ions in the interaction region were extracted towards the ion momentum spectrometer by an applied pulsed electric field, according to each electron detection. The electron pass energy of the DTA was set to 200 eV, and the corresponding energy resolution was ~1.9 eV. The photon energy used for Cl 2p core ionization was 220 eV.

Figure 1(a) shows the total Auger spectrum and coincidence Auger spectrum after the Cl 2p core ionization of CH_3Cl. The coincidence spectrum is extracted from the total Auger spectrum, using the time-of-flight information of H_3^+. The vertical lines above the experimental data are the theoretically calculated Auger final states, along with their valence electron configuration, which are listed on the right. The coincidence Auger spectrum has a single peak at ~31 eV, which is hardly observed in the case of the C 1s core ionization [4]. This indicates that the H_3^+ formation process occurs site-specifically through the Cl 2p core ionization, with a relation with the $3e^{-2}$ Auger final states. To give further insight into the molecular dynamics of the dissociation mechanism of H_3^+, a comparison experiment was conducted, using deuterated chloromethane, CD_3Cl. Figure 1(b) shows the total Auger and coincidence Auger spectra after the Cl 2p core ionization of CD_3Cl. The coincidence Auger spectrum in Fig. 1(b) has a similar spectral profile compared to the CH_3Cl case in Fig. 1(a), where the only difference seen is the lower coincidence detection rate of the D_3^+ fragment ions. The similar spectral profile strongly suggests the same $3e^{-2}$ Auger final states involved in the dissociation mechanism. Furthermore, because the deuterium atom is twice as heavy than the hydrogen atom, molecular motion around the deuterium atom is repressed. The lower abundance of D_3^+ implies that molecular deformation due to vibrational motion around the C-D bond is suppressed, which resulted in decreasing the abundance of D_3^+.

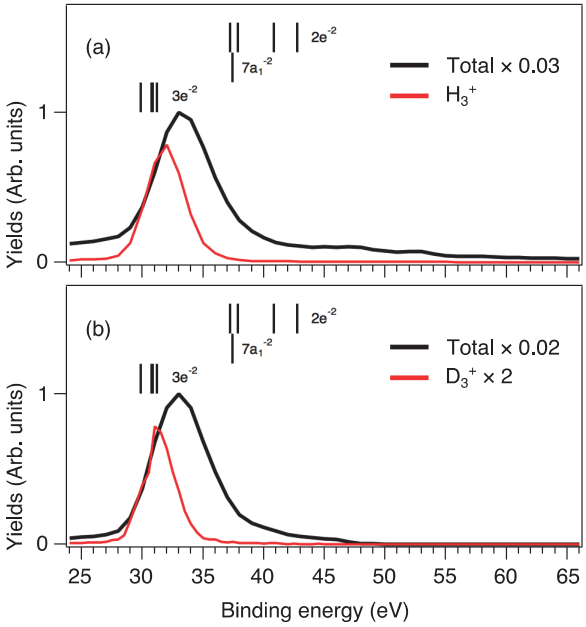

Fig. 1. Total Auger spectra (black) and coincidence Auger spectra (red) following Cl 2p core ionization from (a) CH_3Cl and (b) CD_3Cl.

[1] J. H. D. Eland, Rapid Commun. Mass Spectrom. **10** (1996) 1560

[2] S. Pilling *et al.,* Mon. Not. R. Astron. Soc. **375** (2007) 1488.

[3] K. Hoshina *et al.*, J. Chem. Phys. **129** (2008) 104302.

[4]H. Iwayama and E. Shigemasa, UVSOR Activity Report 2015 **43** (2016) 107.

BL6U

Intermolecular Coulombic Decay of Core Excited Nitrogen Molecular Clusters

H. Iwayama[1, 2]

[1]*UVSOR Synchrotron Facility, Institute for Molecular Science, Okazaki 444-8585, Japan*

[2]*School of Physical Sciences, The Graduate University for Advanced Studies (SOKENDAI), Okazaki 444-8585, Japan*

Intermolecular Coulombic decay is an efficient electronic relaxation of excited molecules placed in a loosely bound chemical system (such as a hydrogen bounded or van-der-Waals-bounded cluster). This decay process ionize neighboring molecules to excited one and eject low-enegy electrons, which play an important role in DNA damage induced ionizing radiation. Recently, it was proposaled that emission site and energy of the electron released during this process can be controlled by coupling the ICD to a resonanct core excitation [1]. These properties may have consequences for fundmental and applied radiation biology. In this work, we investigated ICD process of core excited nitrogen molecule clusters by using Auger-electron ion coincidence technique. Since ICD process lower the double ionization threshold, we measured binding energy of Auger states corresponding to double ionizations. Compared to isolated nitrogen molecules, we observed lowering of double ionization threshold for nitrogen molecular clusters.

The Auger-electron-ion coincidence measurements were performed on the undulator BL6U at UVSOR. The Auger electrons and product ions were measured in coincidence by a double toroidal electron analyzer (DTA) and an ion momentum spectrometer, respectively. The pass energy of DTA was set to 400 eV. All signals from the ion and electron delay-line detectors were recorded with an 8ch TDC board. The photon energy was tuned to 401.1 eV, which corresponds to the resonance energy of the N 1s $\rightarrow\pi^*$ excitation for isolated and clustered nitrogen[1]. Nitrogen clusters were produced by supersonic expansion through a 100-μm nozzle at 220K. The stagnation pressure is 8 bar. The average cluster size was estimated to be ~10 molecules per cluster.

Figure 1 shows time-of-flight mass spectra for (a) molecular nitrogen and (b)clustered nitrogen. For molecular nitrogen, we observed parent molecular ions of N_2^+ and fragment ions of N^+. For clustered nitrogen, we observed cluster fragment ions of $(N_2)_n^+$ ($n \geqq 2$) and $(N_2)_nN^+$ ($n \geqq 1$) in addition to N_2^+ and N^+ ions.

To investigate double ionization thresholds, we explore the events where we detected two fragment ions in coincidence with an Auger electron. Figure 2 shows Auger spectra in coincidence with two fragment ions for (a)isolated and (b)clustered nitrogen. The binding energy distribution of Auger states resulting in double ionizations for nitrogen molecular clusters are significantly lower than isolated nitrogen molecules. The enhancement around binding energy of 45 eV corresponds to the ICD process of core excited nitrogen molecular clusters. Analysis in more detail is in progress.

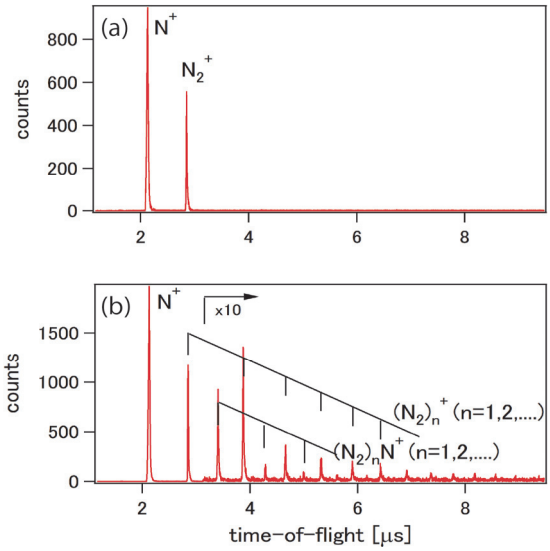

Fig. 1. Time-of-flight mass spectra for (a) N_2 molecules and (b) clusters.

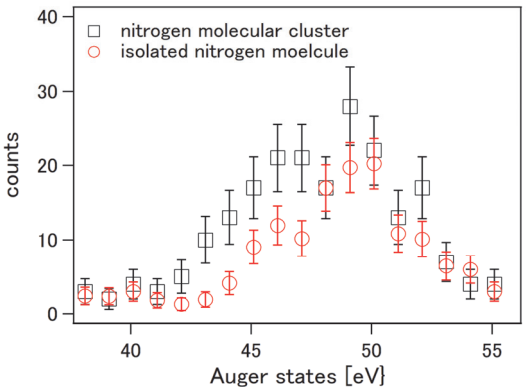

Fig. 2. Coincidence Auger spectra with two fragment ions for nitrogen molecules and clusters.

[1] K. Gokhberg, *et al.,* Nature **505** (2014) 661.
[2] R. Flesch, *et al*., Phys. Rev. Lett. **86** (2001) 3767.

BL6B

Microfluidics of Liquid Mixtures for Infrared Microscopy

M. Nagasaka[1, 2], A. A. Vu[1, 3], H. Yuzawa[1], N. Takada[1], M. Aoyama[1], E. Rühl[3] and N. Kosugi[1, 2]

[1]*Institute for Molecular Science, Okazaki 444-8585, Japan*

[2]*SOKENDAI (The Graduate University for Advanced Studies), Okazaki 444-8585, Japan*

[3]*Physikalische Chemie, Freie Universität Berlin, Takustr. 3, D-14195 Berlin, Germany*

Microfluidics is a chemical technique to realize highly efficient chemical reactions in the liquid phase [1]. Recently, X-ray diffraction in the hard X-ray regime has been used for a variety of systems by using microfluidics [2]. Previously, we applied infrared (IR) microscopy to characterize microfluidic flows [3], but the microfluidic channel was not completely sealed at that time. Recently, we have improved the microfluidic cell for soft X-ray absorption spectroscopy and successfully observed a laminar flow in the mixed part of the microfluidic system [4]. In this study, we have used it for IR microscopy.

The experiments were performed by using the IR microscopy setup IRT-7000 at BL6B. A T-shape microfluidics setup with the width of 50 μm is made from PDMS resin which is covered by a 100 nm Si_3N_4 membrane. The spatial resolution of 30 × 30 μm^2 is reached by using a ×16 Cassegrain mirror. IR spectra are taken by detecting the reflected infrared light by an MCT detector.

Figure 1 shows IR spectra of pyridine and water taken from the mixed part of the microfluidic cell, at positions shown in Fig. 2. The IR spectra correspond to the OH stretching vibration of water around 3392 cm^{-1} and the CH stretching vibration of the pyridine ring around 2936 cm^{-1}, respectively. The absorbance of water and pyridine at different positions is obtained from the fitting results of the IR spectra to both the vibrational peaks.

Figure 2(a) shows the 2D image of the absorbance of water. Pyridine (*P*) flows from the upper side, and water (*W*) from the lower side. The water-pyridine mixture (*M*) flows to the right-hand part after the junction of the liquids. In the mixed part of the microfluidic flow, the absorbance of water shows high intensity at Y = 120 μm. On the other hand, Figure 2(b) shows the 2D image of the absorbance of pyridine, which shows high intensities at Y = 150 μm. These results suggest that the mixed part of the microfluidic flow is evidently laminar between Y = 120 and 150 μm. IR microscopy enables us to observe both chemical compounds separately by selecting their respective vibrational modes.

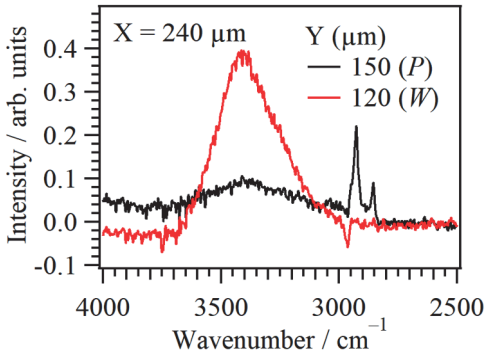

Fig. 1. IR spectroscopy of pyridine (*P*) and water (*W*) in the mixed part of the T-shape microfluidic cell, at positions shown in Fig. 2.

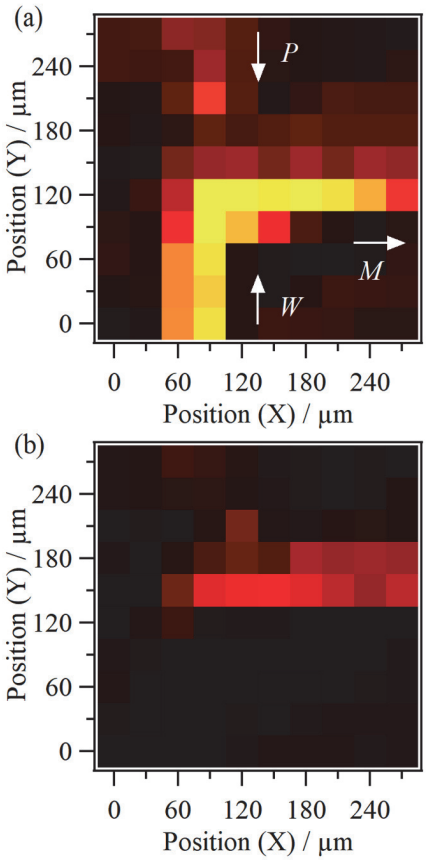

Fig. 2. The 2D images of the absorbance of (a) water and (b) pyridine in the T-shape microfluidic cell obtained from IR spectra at different positions.

[1] T. Kitamori *et al.*, Anal. Chem. **76** (2004) 53.
[2] B. Weinhausen and S. Köster, Lab Chip **13** (2013) 212.
[3] M. Nagasaka *et al.*, UVSOR Activity Report **2016** (2017) 116.
[4] M. Nagasaka *et al.*, in this volume.

UVSOR User 4